

MIT Open Access Articles

An Articulating Tool for Endoscopic Screw Delivery

The MIT Faculty has made this article openly available. **Please share** how this access benefits you. Your story matters.

Citation: Petrzelka, Joseph E. et al. "An Articulating Tool for Endoscopic Screw Delivery." Journal of Medical Devices 5.1 (2011): 011004.

As Published: <http://dx.doi.org/10.1115/1.4003435>

Publisher: American Society of Mechanical Engineers

Persistent URL: <http://hdl.handle.net/1721.1/68644>

Version: Author's final manuscript: final author's manuscript post peer review, without publisher's formatting or copy editing

Terms of use: Creative Commons Attribution-Noncommercial-Share Alike 3.0



AN ARTICULATING TOOL FOR ENDOSCOPIC SCREW DELIVERY

(MED-10-1046)

Joseph E. Petrzelka

Massachusetts Institute of Technology
77 Massachusetts Ave 35-135
Cambridge, MA 02139
jepetrz@mit.edu

Manas C. Menon

Massachusetts Institute of Technology

Clara J. Stefanov-Wagner

Massachusetts Institute of Technology

Suresh K. Agarwal, MD

Boston University

Dimitris Chatzigeorgiou

Massachusetts Institute of Technology

Michelle Lustrino

Massachusetts Institute of Technology

Alexander H. Slocum, PhD

Massachusetts Institute of Technology

ABSTRACT

This paper describes the development of an articulating endoscopic screw driver that can be used to place screws in osteosynthetic plates during thoracoscopic surgery. The device is small enough to be used with a 12 mm trocar sleeve and transmits sufficient torque to fully secure bone screws. The articulating joint enables correct screw alignment at obtuse angles, up to 60° from the tool axis. A novel articulating joint is presented, wherein a flexible shaft both transmits torque and actuates the joint; antagonist force is provided by a super-elastic spring. Screws are

secured against the driver blade during insertion with a retention mechanism that passively releases the screw once it is securely seated in the bone. The prototype has been fitted with a blade compatible with 2.0 and 2.3 mm self-drilling screws, though a different driver blade or drill bit can be easily attached. Efficacy of the tool has been demonstrated by thoracoscopically securing an osteosynthetic plate to a rib during an animal trial. This tool enables minimally invasive, thoracoscopic rib fixation.

INTRODUCTION

An articulating tool for endoscopic placement of screws will enable minimally invasive internal fixation of rib fractures using video-assisted thoracic surgery (VATS). VATS is a well-established procedure for pulmonary resection, lung volume reduction, lung biopsy, and pericardial resection. By selectively ventilating one lung, much of the pleural cavity becomes accessible; an appropriate device for screw delivery enables VATS fixation of rib fractures using osteosynthetic plates.

Multiple fractures in adjacent ribs compromise thoracic stability and result in paradoxical motion (*flail chest*) during respiration. This condition is common; 4-10% of trauma patients have rib fractures, of which 10-15% exhibit paradoxical motion [1]. This condition is painful at best, but also reduces respiratory efficacy; in extreme cases the fracture endangers the integrity of the lungs or heart. Chest wall instability can be treated by sedation of the patient or through artificial respiration, though internal fixation (placement of an osteosynthetic device) is often required. Nirula *et al.* [2] identify three cases in which fixation may be beneficial: (1) in the case of multiple fractures and paradoxical motion, (2) in the case of isolated fractures that result in significant pain, and (3) in the case of a previous fracture that has failed to heal. Engel *et al.* [1]

describe a survey of literature that demonstrated shorter ventilation times and ICU stays in *all cases* where internal fixation was used. Solberg *et al.* [3] report that internal fixation reduces ventilation time, ICU stay, and sepsis.

Despite the clear benefits of internal fixation, existing procedures are so invasive that many surgeons opt to treat indications with ventilation and analgesia alone. Titanium osteosynthetic plates are perhaps the most prevalent fixation method in the literature; Nirula *et al.* [2] regard these as the standard against which other methods must compare. These plates are screwed to the anterior surface of the rib at each fracture site, requiring large incisions and separation of musculature. Acute Innovations recently introduced a U-plate design advertised as minimally invasive, though the device still requires a large incision, considerable dissection, and significant separation of musculature [4,5]. Literature in the field has called for further advances in minimally invasive procedures [2].

Performing internal rib fixation thoracoscopically would provide three distinct advantages. First, this approach eliminates the large incisions and separation of musculature required for existing techniques. Second, a mechanical advantage is obtained; a fracture constrained on the proximal surface will be placed in compression during normal respiratory stresses, offering greater stability and eliminating stress shielding; to support this hypothesis, we note that the radius of curvature of the ribcage increases during respiration [6], while previous biomechanical tests have simulated loading in a consistent manner [5]. Third, the neurovascular bundle along the inferior edge of each rib is clearly visible during VATS placement such that the surgeon can avoid nerve contact and associated post-operative pain, which is a major driver for post-operative removal of implants.

In this paper, we present a new articulating tool for enabling a VATS procedure for rib fixation. This tool can both drill the rib cortex and deliver self drilling or self tapping screws. We are aware of no prior art that accomplishes this result. The literature supports the use of ductile mandibular plates for fixation [1], a method preferred by the authors. In a VATS procedure, these plates can be delivered through small incisions using existing endoscopic tools. In this presentation, we focus exclusively on a novel device that can secure these plates using self-drilling bone screws.

The following sections will present the specific requirements for an endoscopic drill and screw delivery device. Next, an overview of the device design is presented followed by engineering details of each component. A scale prototype is shown, and finally we demonstrate the efficacy of the device in a porcine trial.

DEVICE REQUIREMENTS

Placement of osteosynthetic plates in a VATS procedure requires an articulating endoscopic tool to drill or drive monocortical self-drilling or self-tapping screws. In this section, we discuss specific requirements for (1) an endoscopic device, (2) an articulating joint designed for the thoracic cavity, (3) a device for driving bone screws, and (4) a screw retention mechanism.

The end of the tool must be able to pass through a standard trocar sleeve at the site of incision. While a smaller trocar sleeve (and thus smaller tool) is clearly advantageous, we consider the case of a large 12 mm trocar sleeve. Hence, the tool must fit through a cylindrical opening 12 mm in diameter. Further, materials must be selected to be both (1) bio-inert and (2) resistant to high temperatures during autoclave sterilization.

The tool must articulate to drill or allow placement of screws normal to the local surface of a curved rib. The end length of the tool (from the articulation joint to the tip of the driver) is directly related to the angle through which the same end must articulate (Fig. 1). A shorter end length results in a smaller degree of articulation and improved maneuverability in the thorax, but a minimum length is imposed by the components that must be included. The minimum radius of curvature of the ribs imposes an upper limit on tool end length; from Mohr *et al.* [7] this is approximately 10 cm in adults. From the authors' surgical experience and benchmark relative to endoscopic staplers, 6 cm would result in a maneuverable tool. Assuming an end length of 6 cm, the tool end must articulate between neutral and 60°. The symmetry of the device allows this one direction of articulation to reach a partial hemisphere of screw orientations. From parametric modeling of rib geometry (data from [7]), 60° will allow full access to multiple anterior fractures through a single posterior incision. The articulation must have a resolution of at least 10° (the accuracy with which screws must be placed; [8]). This end length and level of articulation is comparable to those of conventional endoscopic staplers [12].

To start a drill or screw into the rib cortex, a normal thrust force of 15 N must be exerted at the tip of the driver, representing the maximum normal force the tool will experience. Kincaid *et al.* [9] report starting loads on the order of 25 N for 3.5 mm self-tapping screws. Hillery and Shuaib [10] show thrust forces between 25 and 45 N for a 3.5 mm drill in cortical bone, depending on drill feed. In the authors' experience, self-drilling screws require very little thrust force to start driving (an order of magnitude less than the results reported here). Still, we obtain a conservative estimate by scaling the results in the literature for a 2.0 mm screw; this allows adaptation of the device to drilling or self-tapping screw applications.

Hitchon *et al.* [11] find that the torque required to drive a 4 mm self-drilling screw in vertebrae is approximately 0.5 Nm, even at high bone mineral densities. Kincaid *et al.* [9] report similar values for 3.5 mm monocortical self-tapping screws in femurs. In comparison, drilling requires much less torque; Hillery and Shuaib [10] report values of 0.010 to 0.015 Nm for a 3.2 mm drill. Scaling these values linearly results in a torque requirement of approximately 0.25 Nm for a 2.0 mm screw. This scaling is quite conservative since the cortex of ribs is much thinner than that of constructs tested in the literature.

Finally, to avoid the loss of screws inside the body, the tool must actively retain the screw, at least on the order of magnitude of other forces (e.g. thrust force).

BACKGROUND

To the authors' knowledge, no device exists in prior art that satisfies the requirements set forth. While a variety of endoscopic tools are commercially available, few allow active tool articulation (e.g. Oberlin and Penrod [12], Nicholas *et al.* [13]) and none of these provide torque transmission.

Flexible shaft screw drivers are available for automotive and surgical use; patents by Prager and Volzow [14], Beyar and Sohn [15], and McGuire [16] use flexible shafts in surgical screw drivers, though their devices are either fixed-angle or unconstrained and thus unable to maintain a specific degree of articulation. Takehana *et al.* [17] use closed-loop control of shape memory alloy elements to direct the lens of a laparoscope, but their invention would be incapable of transmitting the high axial forces required for screw placement.

Devices for surgical screw placement commonly incorporate a screw holder of the type described by Stihl [18]; while this design is robust, it requires external actuation and is difficult to incorporate into an articulating device (Fig. 2). Schwager and Dorawa [19] describe another mechanical screw retention device, also requiring external actuation.

We conclude that there are no existing mechanisms which accomplish the requirements of endoscopic screw placement.

DEVICE DESIGN

Our endoscopic screwdriver (Fig. 3) incorporates three degrees of freedom. Primarily, continuous (infinite) rotary motion must be provided at the tip of the screw. Second, an articulating joint must provide small angle rotations (0° to 60°). Third, a positive screw retention device must be actuated in a linear manner.

Rotary motion is provided via a flexible shaft that ‘floats’ through the articulating joint area. The joint pivots about two symmetric pins. Changing the arc length of the flexible shaft actuates the joint, with antagonist motion provided by a super-elastic spring. While the flexible shaft runs along the axis of the device, the hinge pins are offset slightly to avoid a singularity at the neutral position. This arrangement is particularly desirable because it requires that only two components – the flexible shaft and the spring – pass through the hinge region. Further, the flexible shaft serves a dual role: it both transmits torque and controls articulation. This mechanism is illustrated in Fig. 4.

A novel screw retention mechanism is located at the end of the shaft. This design uses an under-sized but compliant ring to hold the screw against the driver head; as the screw fully seats it pulls itself through the compliant ring to a released position. In this manner, the mechanism is passive and does not require external actuation (Fig. 5).

A drive module is connected to the articulating head via a tubular housing, through which a drive shaft passes. The drive module uses a DC motor to apply torque, though an alternative embodiment could allow manual or pneumatic power sources. A lead screw collar changes the location of the housing with respect to the drive shaft, in effect changing the arc length of the flexible shaft and the angle of articulation (Fig. 6).

The following sub-sections discuss the specific mechanical element selection and modelling for each module: torque transmission, joint actuation, screw retention, and user control.

Torque Transmission

The primary function of the device is to drill or drive a screw, requiring a transmission of torque. Further, this torque must be transmitted through a 60° variable-angle joint. From a survey of literature, we identify that 0.25 Nm is sufficient to drive a 2.0 mm self-drilling screw; less torque is required for driving a self-tapping screw or for drilling. We designed a device capable of providing 1.0 Nm, allowing for a generous safety factor. Further, the transmission element must consume only a fraction of the 12 mm envelope to allow for the fitting of other components (e.g. hinge and actuation elements).

Rigid mechanical elements are unable to transmit the required torque at the small scale desired. Variable-angle gear sets are limited by both relative cost and size. A universal joint (U-joint)

seems a natural choice for variable-angle torque transmission. The use of two serial U-joints results in constant velocity (impossible using a single U-joint) and requires each to flex only 30°. However, at the small diameters required, U-joints have detrimentally low torque ratings. A survey of commercially available stainless steel U-joints shows that a prohibitively large component would be required to achieve a reasonable design safety factor (Fig. 7).

A compliant element offers much higher torque transmission at small scales. Flexible shafts (flex shafts), wherein a cable core provides high torsional stiffness but low bending stiffness, offer an alternative to gear and U-joint systems. To our advantage, flex shafts are limited only by their bend radius rather than by their absolute angle; thus, achieving a 60° bend is quite feasible. Further, flex shafts are capable of transmitting much higher torques than U-joints at the millimeter scale. The primary failure mode of a flex shaft is not shear, but rather elastic instability via helixing. The critical torque T_c at which the flex shaft becomes unstable is determined by its bending stiffness B , free length ℓ , and tension P [20]:

$$T_c = 2\sqrt{\frac{B^2\pi^2}{\ell^2} + BP} \quad (1)$$

Due to advantages of higher torque ratings at small size scales, this tool uses a 3.3 mm flex shaft with a 50 mm minimum bend radius and a 3.4 Nm maximum torque; testing shows that zero-tension helixing occurs at T_c of about 1 Nm. The bend radius of this shaft dictates the required free length; to a first order (Fig. 8), one can show that

$$R = L \cot \frac{\theta}{2} - D \quad (2)$$

and thus determine the free length, $\ell = 2L$, as a function of the maximum angle of articulation θ and minimum bend radius R . Hence, for our device, a free length ℓ of about 60 mm is required (note that this corresponds to $L = 30$ mm, which only consumes half of the maximum end length of 6 cm, leaving room for bushings and a driver blade). Further, the distance that the shaft moves from neutral is

$$d = L \left[1 - \cos \frac{\theta}{2} \right] / \left[\sin \frac{\theta}{2} \right] \quad (3)$$

In the present embodiment, this results in a deflection d of 8 mm, requiring that a channel be provided such that the shaft can flex a small distance outside the tool housing at full articulation. At a neutral position (zero degrees articulation) the shaft is fully within the tool housing for movement through a trocar sleeve (Fig. 4).

Joint Actuation

As a secondary function, the device must articulate between zero and sixty degrees; the mechanism of actuation is not a trivial design problem given the size constraints and anticipated forces. A four-bar linkage would allow fully actuated control of the articulation angle, but at this small scale link buckling and pin shear become problematic. To solve these problems, we developed an under-actuated design that utilizes a tensile element coupled with an antagonist spring.

The flexible shaft acts as the tensile element necessary to actuate the joint. Based on Eqn. 2 and Fig. 8, the arc length of the flexible shaft is a function of articulation angle θ :

$$S = \theta \left[L \cot \frac{\theta}{2} + D \right] \quad (4)$$

Alternatively, the articulation angle can be expressed as a function of shaft arc length, thus allowing a deterministic change of articulation angle by modifying the relative position of the tool housing and flexible shaft. This relationship can be observed in Fig. 9; note the different locations of the flexible shaft driven end at the extremes of articulation. To avoid a singularity at $\theta = 0$, the pivot point of the joint is placed slightly above the centerline of the flexible shaft (distance D in Fig. 8).

The size constraints of this device motivate selection of a super-elastic nitinol (NiTi) antagonist spring. An ideal antagonist device would provide a force of the same magnitude as the thrust force (15 N) along the entire range of articulation. Constant force springs made from standard materials (i.e. spring steels) are too weak at the scale required. The force exerted by a cantilevered beam spring configuration is governed by beam bending theory and is proportional to the curvature, ρ , and radius, r , which are related to the yield strain according to

$$r = \varepsilon_{yield} / \rho_{max} \quad (5)$$

The curvature ρ_{max} is dictated by design geometry (similar to Eqn. 2); hence this configuration results in an extremely small spring diameter and low forces for conventional materials. However, the super-elastic properties of NiTi provide a yield strain (ε_{yield}) that is an order of magnitude greater than conventional materials, while maintaining a relatively constant stress level ($\sigma_{superelastic}$). Thus, the use of a NiTi beam spring allows a significant antagonist force in a

small envelope. Moreover, the NiTi response is relatively constant above 10 degrees of articulation, whereas traditional materials exhibit a linear response; this constant force results in a more predictable response to external stimuli during use (Fig. 10).

Hard stops are incorporated in the housing design at each extreme to prevent over-articulation of the joint in this under-actuated configuration.

To validate this design, each structural force and tension were computed as a function of articulation angle θ . These calculations show that the shear force on the pin joint, the flexible shaft tension, and the actuation force are nearly identical (Fig. 11). Each of these forces are well below the yield point of their respective mechanical elements.

Screw Retention

While a variety of screw retention devices exist in current art, each requires actuation of some variety. Due to the limited space available in the articulating joint, a passive device is preferred. To this end, a sliding sleeve is installed at the driver tip of the device. This sliding sleeve, with the screw pre-attached, snaps onto the driver tip (Fig. 5). When axial loading between the screwdriver and the rib surface reaches a critical threshold (order of 10 N), the screw snaps free as the sleeve slips backwards.

Both ends of the retainer (screw and tool) employ cantilever snap fits (Fig. 5), though the axisymmetric design we employ is not easily modeled by standard snap fit methods. To model these snap fits analytically, we use energy methods to balance the removal force, beam deflection, and friction. To calculate the stiffness of the cantilevers, we make thin shell approximations.

Testing of our design demonstrates that reasonable radial forces (of order 10 N) fail to dislodge the screw from this retention device, thus ensuring that the screw will not fall off inadvertently during surgery. Furthermore, we have tailored the design for low application force (to facilitate screw alignment to the driver tip) and moderate removal force.

User Control

A handle is incorporated to allow device control outside the body. This grip must provide a means of (1) applying torque and (2) actuating the wrist.

Torque can be applied via a number of equally acceptable methods, including manual, electric, or pneumatic drives. Any powered drive must have a peak torque on the order of 1 Nm and be able to operate between 10 and 1000 rpm for combined drilling and driving functions. In the embodiment presented here, we provide an adapter for a standard surgical drill, though early prototypes utilized both manual and integral DC gear motor drives. We have found that limiting current provides an effective means of preventing over-torque.

Articulation is controlled by changing the relative position of the drive shaft (coupled to the flex shaft) and the main housing; this is accomplished by turning a leadscrew collar located at the handle of the tool. The total movement required follows from the change in arc length (Eqn. 4):

$$\Delta S = 2L - \theta \left[L \cot \frac{\theta}{2} + D \right] \quad (6)$$

In the present design, ΔS of 6 mm is required for articulation of 60°. While a number of mechanisms could accomplish this, a nut / leadscrew combination is chosen for fine resolution and stability (assuming it cannot be backdriven). The drive shaft is axially constrained in the

handle so that its axial tension is decoupled from the drive mechanism. Feedback is provided either through visual inspection of the articulating end or by incorporating a rule into the grip that correlates ΔS with θ .

PROTOTYPE / TESTING

Several prototypes have been constructed and tested to demonstrate that each design criterion was met. Both benchtop and porcine cadaver trials have demonstrated the efficacy of the tool. The design and actuation of the articulating mechanism proved intuitive to first-time users in the surgical community.

The novel articulating elbow and preferred handle embodiment were prototyped for testing (Fig. 13). Each housing at the articulating joint was machined from stainless steel; the majority of other internal components were manufactured from various stainless steel alloys (e.g. flex shaft, drive shaft, pivot pins, primary housing). Rulon 641 bushings were used at each end of the flex shaft for biocompatibility and autoclave temperature resistance. The handle was constructed an anodized aluminum leadscrew collar and a series of stainless steel sleeves designed to fit to a standard reaming attachment for the Stryker Cordless Driver series of battery tools. A miniature collet was fitted to the end of the flex shaft to allow interchange of drill and driver bits.

The end of the tool easily fits through a 12 mm trocar. The angle of articulation can be adjusted continuously between 0° and 60° by turning the lead screw nut (Fig. 14). The total end length of the device is approximately 5 cm from the articulating joint to the driver tip.

Prototypes of the screw retainer were machined from Delrin to the specifications set from the previous analysis. In benchtop testing, these prototypes demonstrated easy placement with a relatively stiff grasp on the screw.

Two separate porcine trials have been conducted [21]. The first demonstrated the ability of this design to enter through a trocar and be manipulated to a series of different operative sites. The second demonstrated effective placement of osteosynthetic plates and screws (Fig. 15). In this procedure, we were able to both drill and place screws with the same tool operating at different speed ranges. Using the screw retainer allowed both reliable delivery of screws and manipulation of plate position with the screw tip. Screws were successfully removed using a bare driver tip without the screw retainer and using forceps for retrieval from the thoracic cavity.

CONCLUSION / FUTURE WORK

In this work we presented a new device for endoscopic screw placement. This tool enables exploration of new methods for internal fixation of rib fractures, using well established VATS procedures. Using a novel articulating joint, the device can place screws at obtuse angles (up to 60° off-axis) to meet the local curvature of ribs while delivering relatively high levels of torque. The device can easily be adapted to other surgical applications by attaching different driver trips or drill bits. A scale prototype proves design feasibility. Using the tool in a porcine model demonstrated promising results for VATS fracture stabilization.

While this tool has provided promising results in preliminary tests, we note that significant research remains to develop a complete clinical solution; we defer a thorough discussion of clinical aspects to forthcoming publications (including [21]). Our future endeavors include testing in cadaver models with flail chest segments to evaluate the ability to reduce fractures and

the mechanical stability of the stabilized construct. Development is ongoing in specific systems for fracture reduction, implant delivery, and implant removal.

ACKNOWLEDGEMENTS

This device was developed as a term project in MIT Course 2.75: Precision Machine Design. We are grateful to Lynn Osborn and Dr. Tom Brady of *The Center for Integration of Medicine and Innovative Technology* (www.cimit.org) for providing support for Course 2.75 and this project (DOD funds, FAR 52.227-11). We are also grateful to the Boston University School of Medicine, Conor Walsh, and Nevan Hanumara for their support and guidance throughout the project. Finally, we thank SolidWorks Corporation for providing solid modeling software.

REFERENCES

- [1] Engel, C., Krieg, J.C., Madey, S.M., Long, W.B., and Bottlang, M., 2005, “Operative Chest Wall Fixation with Osteosynthesis Plates,” *Journal of Trauma*, 58(1), pp. 181-186.
- [2] Nirula, R., Diaz, J.J., Trunkey, D.D., and Mayberry, J.C., 2009, “Rib Fracture Repair: Indications, Technical Issues, and Future Directions,” *World Journal of Surgery*, 33(1), pp. 14-22.
- [3] Solberg, Moon, Nissim, Wilson, and Marquies, 2009, “Treatment of Chest Wall Implosion Injuries without Thoracotomy: Technique and Clinical Outcomes,” *Journal of Trauma*, 67(1), pp. 8-13.
- [4] *RibLoc*, 2009, Accute Innovations, < <http://www.acuteinnovations.com/Products/RibLoc> >, accessed November 2009.

- [5] Sales, Ellis, Gillard, Liu, Chen, Ham, and Mayberry, 2008, "Biomechanical Testing of a Novel, Minimally Invasive Rib Fracture Plating System," *Journal of Trauma*, 65(5), pp. 1270-4.
- [6] DeGroot, A., Wantier, M., Cheron, G., Estenne, M., and Paiva, M., 1997, "Chest wall motion during tidal breathing," *Journal of Applied Physiology*, 83, pp. 1531-7.
- [7] Mohr, M., Abrams, E., Engel, C., Long, W.B., and Bottlang, M., 2007, "Geometry of Human Ribs Pertinent to Orthopedic Chest-Wall Reconstruction," *Journal of Biomechanics*, 40, pp. 1310-17.
- [8] Wolter, D., 2001, *Fixation System for Bones*, US 6,322,562.
- [9] Kincaid, B., Schroder, L., and Mason, J., 2007, "Measurement of Orthopedic Cortical Bone Screw Insertion Performance in Cadaver Bone and Model Materials," *Experimental Mechanics*, 47, pp. 595-607.
- [10] Hillery, M.T., and Shuaib, I., 1999, "Temperature Effects in the Drilling of Human and Bovine Bone," *Journal of Materials Processing Technology*, 92, pp. 302-8.
- [11] Hitchon, P.W., Brenton, M.D., Coppes, J.K., From, A.M., and Torner, J.C., 2003, "Factors Affecting the Pullout Strength of Self-Drilling and Self-Tapping Anterior Cervical Screws," *Spine*, 28(1), pp. 9-13.
- [12] Oberlin, J.R., and Penrod, M.A., 1998, *Articulated Surgical Instrument with Improved Articulation Control Mechanism*, US 5,725,536.
- [13] Nicholas, D.A., Russell, B.G., Zvenyatsky, B., Matula, P.A., and Remiszewski, S.H., 1996, *Articulating Endoscopic Surgical Apparatus*, US 5,490,819.
- [14] Prager, R. and Volzow, S., 2008, *Screwdriver for Bone Screws*, US 2008/0243436 A1.
- [15] Beyar, M. and Sohn, Z., 2003, *System for Bone Screw Insertion*, US 6,663,642 B2.

- [16] McGuire, D.A., 1995, *Flexible Surgical Screwdriver and Methods of Arthroscopic Ligament Reconstruction*, US 5,464,407.
- [17] Takehana, S., Ueda, Y., Gotanda, M., Sakurai, T., and Adachi, H., 1990, *Apparatus for Bending an Insertion Section of an Endoscope Using a Shape Memory Alloy*, US 4,930,494.
- [18] Stihl, E., 2001, *Screwdriver*, US 6,189,422 B1.
- [19] Schwager, M. and Dorawa, K., 2008, *Bone Screw Holding Device*, US 2008/0269768 A1.
- [20] Black, A. Robert, 1988, "On the Mechanics of Flexible Shafts," *PhD Thesis, Stevens Institute of Technology*.
- [21] Agarwal, S.K., Petrzela, J.E., Menon, M.C., Stefanov-Wagner, C.J., Chatzigeorgiou, D.M., Lustrino, M.E., and Slocum, A.H., 2010, "Thoracoscopic Stabilization of the Chest Wall," *Proceedings of the New England Surgical Society Annual Meeting*.

List of Figure Captions

FIGURE 1 – AN ENDOSCOPIC DRIVER MUST HAVE AN ARTICULATING JOINT TO PLACE SCREWS AT THE CORRECT ORIENTATION; THE REQUIRED ANGLE OF ARTICULATION IS POSITIVELY CORRELATED WITH THE END LENGTH OF THE DEVICE. WHILE ILLUSTRATED HERE IN TWO DIMENSIONS, THE ADDITIONAL DEGREE OF FREEDOM ALLOWS ACCESS OF MULTIPLE FRACTURE SITES ON DIFFERENT RIBS THROUGH A SINGLE INCISION.

FIGURE 2 – PRIOR SCREW RETAINER DESIGN; THE SCREW CAN BE EITHER HELD BY A SET OF RETAINING AND LOCKING SLEEVES (A) OR RELEASED BY SLIDING THE SLEEVES AWAY FROM THE SCREW HEAD (B) [17]. THIS COMMON DESIGN IS DIFFICULT TO ADAPT TO ENDOSCOPIC USE BECAUSE IT REQUIRES ACTUATION.

FIGURE 3 – ARTICULATING ENDOSCOPIC SCREW DRIVER, SHOWN AT MAXIMUM DEGREE OF ARTICULATION.

FIGURE 4 – NOVEL ARTICULATING JOINT DESIGN INCORPORATING ACTUATION VIA A TORQUE-TRANSMITTING FLEXIBLE SHAFT AND ANTAGONIST ACTUATION VIA A SUPER-ELASTIC SPRING (ILLUSTRATED AT THE EACH EXTREME OF ARTICULATION). A SLOT IN THE HOUSING ALLOWS THE FLEXIBLE SHAFT TO MOVE OFF-CENTER AT HIGH DEGREES OF ARTICULATION.

FIGURE 5 – (A) NOVEL PASSIVE SCREW RETENTION MECHANISM DEMONSTRATING THE USE OF A SNAP FIT TO RETAIN THE SCREW TO THE DRIVER TIP. (B) THE RETAINER SNAPS ONTO THE TOOL END AND SNAPS AROUND THE SCREW HEAD TO FIRMLY RETAIN IT. (C) RETAINER IN THE OPERATING POSITION. (D) AS THE SCREW FULLY SEATS, THE RETAINER IS PUSHED BACK BY THE SUBSTRATE TO RELEASE THE SCREW.

FIGURE 6 – EXTERNAL ACTUATION MECHANISM, INCORPORATING (A) A POWER DRILL ADAPTER TORQUE AND (B) A LEAD SCREW COLLAR TO ADJUST THE RELATIVE POSITION OF THE TOOL BODY (C) FORWARD, WHICH CAUSES THE TIP TO ARTICULATE (D) DUE TO THE RELATIVE FORESHORTENING OF THE FLEXIBLE SHAFT.

FIGURE 7 – STATIC TORQUE RATING VS. OUTER DIAMETER FOR STAINLESS STEEL UNIVERSAL JOINTS; CURVE SHOWS A BEST FIT TO DATA POINTS COLLECTED IN A SURVEY OF COMMERCIALY AVAILABLE COMPONENTS.

FIGURE 8 – MODEL OF FLEXIBLE SHAFT GEOMETRY AS A FUNCTION OF ARTICULATION ANGLE θ , PIVOT LENGTH L , AND PIVOT OFFSET D .

FIGURE 9 – SCHEMATIC ILLUSTRATING THE CHANGE IN FLEX SHAFT ARC LENGTH BETWEEN THE EXTREMES OF ARTICULATION; ACTUATION TENSION IN THE FLEX SHAFT IS BALANCED BY AN ANTAGONISTIC BEAM SPRING.

FIGURE 10 – CHART OF ANTAGONIST MOMENT (Nm) AS A FUNCTION OF ARTICULATION ANGLE FOR NiTi AND STAINLESS STEEL BEAM SPRINGS AT A MAXIMUM CURVATURE OF 72 m^{-1} . THE SUPER-ELASTIC NiTi PROVIDES A LARGER AND MORE UNIFORM ANTAGONISTIC MOMENT FOR UNIFORM RESPONSE TO EXTERNAL STIMULI.

FIGURE 11 – CHART OF FLEX SHAFT TENSION (N) AS A FUNCTION OF ARTICULATION ANGLE; PIN SHEAR FORCE AND ACTUATION FORCE ARE OF SIMILAR MAGNITUDE AND RESPONSE.

FIGURE 12 - CANTILEVER BEAM SNAP FITS ON SCREW RETAINER SHOWN IN (A) NEUTRAL POSITION AND (B) SNAP POSITION. (C) ENERGY METHODS ARE USED TO ANALYTICALLY RELATE REMOVAL FORCE TO THE CANTILEVER DEFLECTION FORCE AND INTERFACE FRICTION, THEMSELVES FUNCTIONS OF CANTILEVER STIFFNESS AND DEFLECTION.

FIGURE 13 – (A) PROTOTYPE OF THE ENDOSCOPIC DRIVER: THE ARTICULATING JOINT IS ACTUATED BY THE FLEX SHAFT, WHILE THE REMOTE HANDLE INCORPORATES AN ADAPTER TO A STANDARD SURGICAL DRILL. A COLLAR WITH AN INTEGRAL LEAD SCREW ALLOWS SIMPLE AND PRECISE ADJUSTMENT OF ARTICULATION. (B) TOOL DISASSEMBLES FOR CLEANOUT AND STERILIZATION.

FIGURE 14 – THE TOOL SUCCESSFULLY ARTICULATES FROM 0° (NEUTRAL) TO 60° WITH CONTINUOUS RESOLUTION; ANGLES OF 10° THROUGH 60° ARE ILLUSTRATED HERE.

FIGURE 15 – IMAGES FROM PORCINE TRIAL. (A) DRILLING; (B) SCREW PLACEMENT USING SCREW RETAINER (C) FULL ARTICULATION FOR DRILLING; (D) PLATE PLACEMENT VIA TROCAR.

Fig1.tif

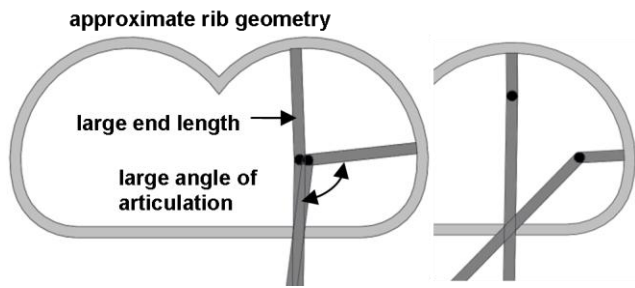


Fig2.tif

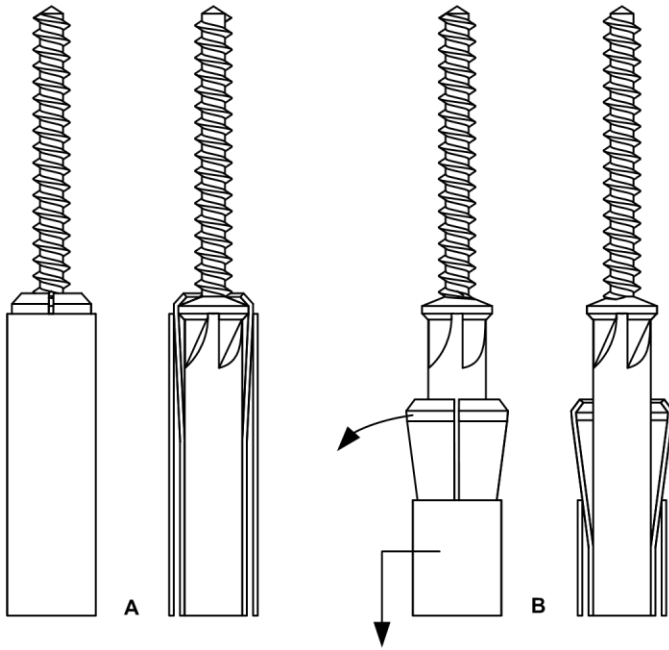


Fig3.tif

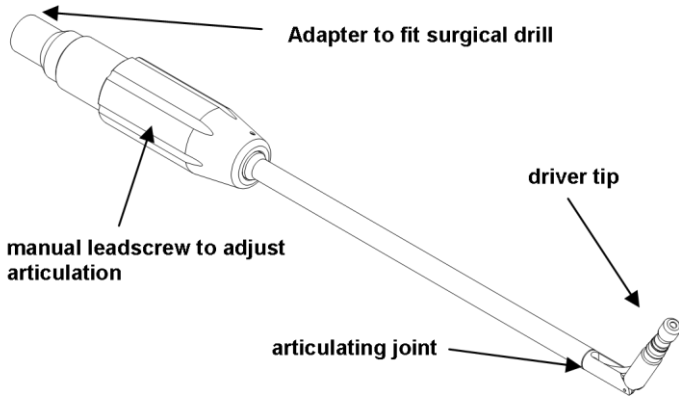


Fig4.tif

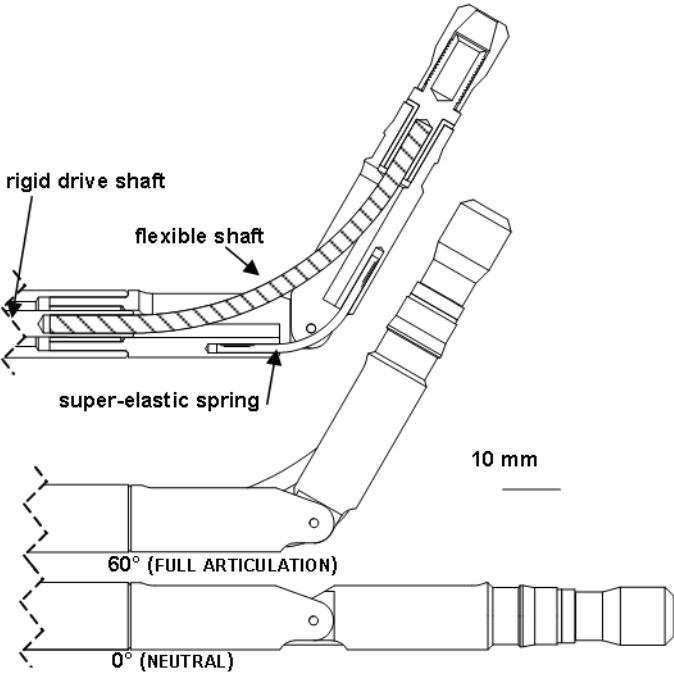


Fig5.tif

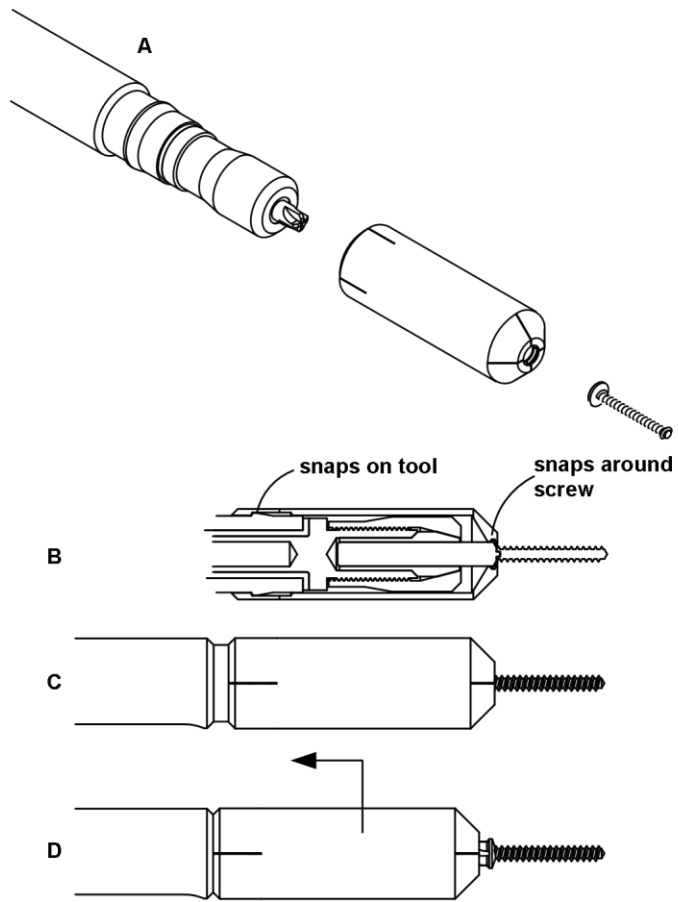


Fig6.tif

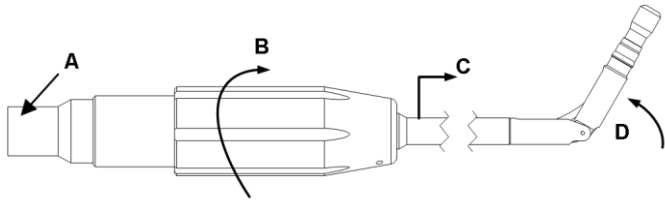


Fig7.tif

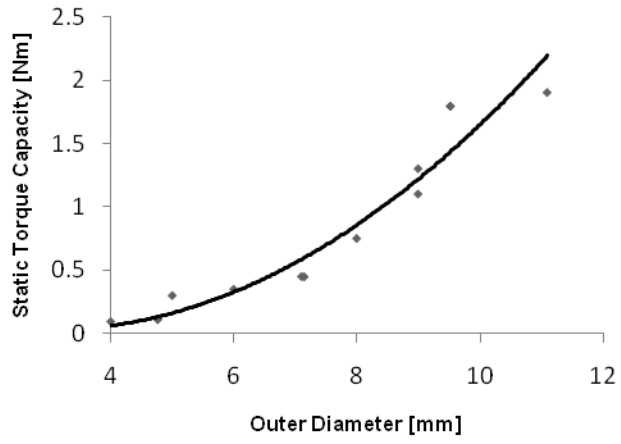


Fig8.tif

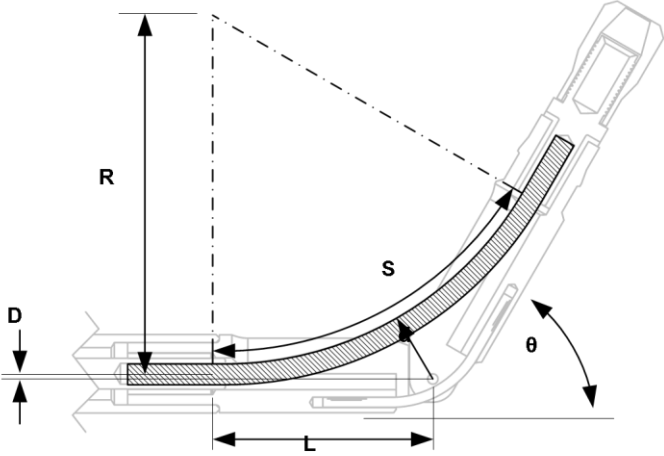


Fig9.tif

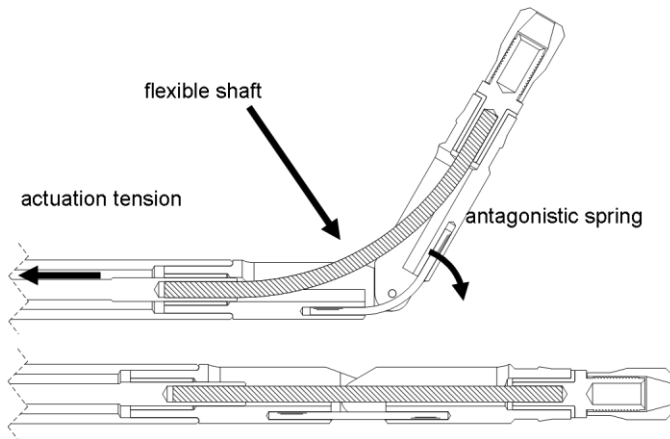


Fig10.tif

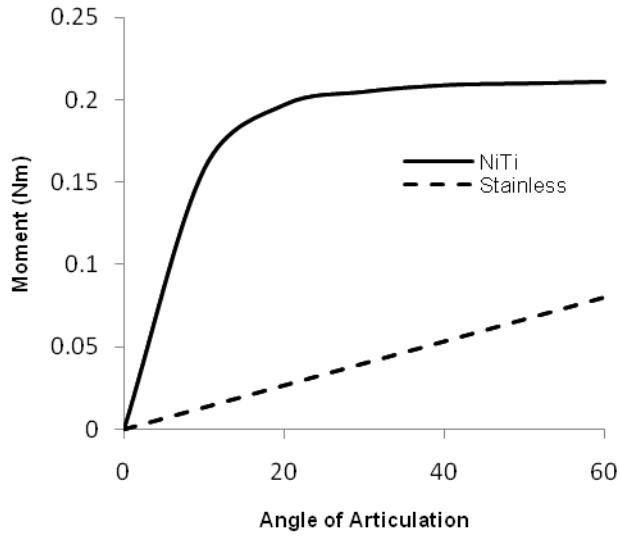


Fig11.tif

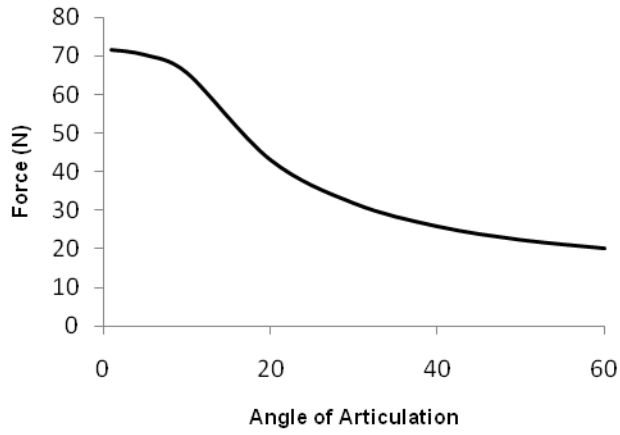


Fig12.tif

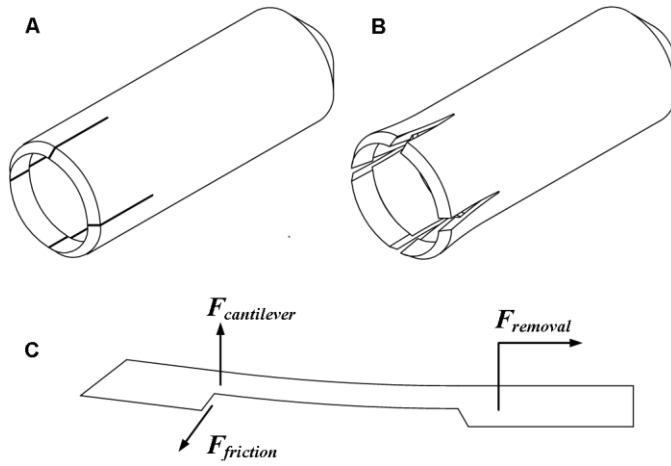


Fig13.tif

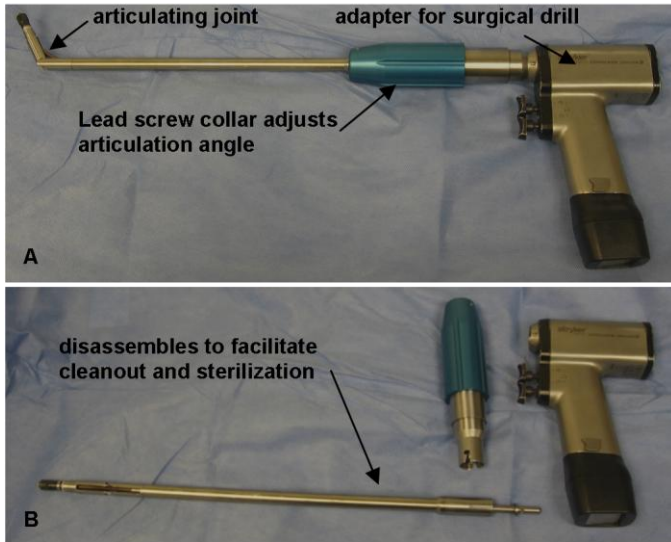


Fig14.tif

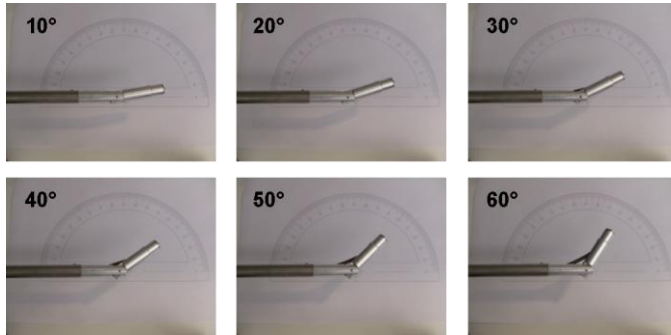


Fig15.tif

